Photochemical & Photobiological Sciences


Volume 1 | Number 1 | Jan 2013 | Pages 1–100

Photochemical & Photobiological Sciences

An international journal

www.rsc.org/pps

ROYAL SOCIETY
OF CHEMISTRY

www.rsc.org/pps

Journal Name RSCPublishing

ARTICLE

Cite this: DOI: 10.1039/x0xx00000x

Received 00th January 2012,
Accepted 00th January 2012

DOI: 10.1039/x0xx00000x

www.rsc.org/

Photoexcited triplet states of UV-B absorbers: ethylhexyl triazone and diethylhexylbutamido triazone

Takumi Tsuchiya,[a] Azusa Kikuchi,*[a] Nozomi Oguchi-Fujiyama,[b] Kazuyuki Miyazawa[b] and Mikio Yagi*[a]

The excited states of UV-B absorbers, ethylhexyl triazone (EHT) and diethylhexylbutamido triazone (DBT), have been studied through measurements of UV absorption, fluorescence, phosphorescence, triplet–triplet absorption and electron paramagnetic resonance spectra in ethanol. The energy levels of the lowest excited singlet (S_1) and triplet (T_1) states and quantum yields of fluorescence and phosphorescence of EHT and DBT were determined. In ethanol at 77 K, the deactivation process of EHT and DBT is predominantly fluorescence, however, a significant portion of the S_1 molecules undergoes intersystem crossing to the T_1 state. The observed phosphorescence spectra, T_1 lifetimes and zero-field splitting parameters suggest that the T_1 state of EHT can be assigned to a locally excited $^3\pi\pi^*$ state within *p*-(*N*-methylamino)benzoic acid, while the T_1 state of DBT can be assigned to a locally excited $^3\pi\pi^*$ state within *p*-(*N*-methylamino)benzoic acid or *p*-amino-*N*-methylbenzamide. The quantum yields of singlet oxygen generation by EHT and DBT were determined by time-resolved near-IR phosphorescence measurements in ethanol at room temperature. EHT and DBT did not exhibit significantly antioxidative properties by quenching singlet oxygen, in contrast to the study by Lhiaubet-Vallet *et al.*

Introduction

Organic sunscreen ingredients act by absorbing UV radiation of sunlight. UV radiation is divided into three ranges: UV-A (320–400 nm), UV-B (280–320 nm) and UV-C (280–320 nm). Historically, one of the most widely used UV-B absorbers in sunscreen formulations has been *p*-aminobenzoic acid (PABA, Scheme 1). PABA was thought to be an effective ingredient, although harmful effects were reported.[1,2] PABA is too water-soluble owing to the presence of the polar amino and carboxyl groups and it can stain clothing and skin.[3] An ideal UV absorber in cosmetic sunscreens should be photostable, water resistant and nontoxic. The most important aspect of an ideal UV absorber is its safety. Therefore the use of PABA has been declining. Nonetheless, PABA continues to appear on the list of approved and permitted sunscreen ingredients in Australia, EU, Japan and USA.[4] PABA has been largely replaced by its derivatives which have better safety profiles and rarely stain skin.[5]

Ethyhexyl triazone (EHT, octyl triazone, Uvinul T150, Scheme 1) is a new UV-B absorber and is included in the list of authorized sunscreen ingredients in Australia, EU and Japan.[4] EHT has a large molecular weight of 823. Larger molecules cannot penetrate into the body and thus cannot act as allergens in man.[6–9] Virtually all common contact allergens have molecular weight of <500.[6,7] EHT possesses multiple chromophores that yield a large molar absorption coefficient of 119 500 mol^{-1} dm^3 cm^{-1} in oil at 314 nm and 134 000 mol^{-1} dm^3 cm^{-1} in methanol at 312 nm.[6,9,10] The low solubility of EHT can be understood as a consequence of the high symmetry.[6]

Diethylhexylbutamido triazone (DBT, dioctylbutamido triazone, Uvasorb HEB, Scheme 1) can be regarded as an improved version of EHT. It is no longer symmetric and the solubility is much higher than EHT.[6] DBT also has a large molecular weight of 766, and a large molar absorption coefficient of 111 700 mol^{-1} dm^3 cm^{-1} in oil at 312 nm.[6] DBT is included in the list of authorized sunscreen ingredients in EU.[4]

In sunscreen formulations, UV absorbers are always combined with other UV absorbers in high concentrations to provide a perfect protection throughout the whole UV radiation range. It is important to determine the energy levels of the lowest excited singlet (S_1) and triplet (T_1) states of individual UV absorbers because the intermolecular energy transfer is one of the most important interactions between the UV absorbers.[11–17] Several studies on the photostability, spectral profile and phototoxicity of EHT and DBT have been reported.[10,18–26] However, to our best knowledge, the energy levels of the excited states of EHT and DBT have not been reported.

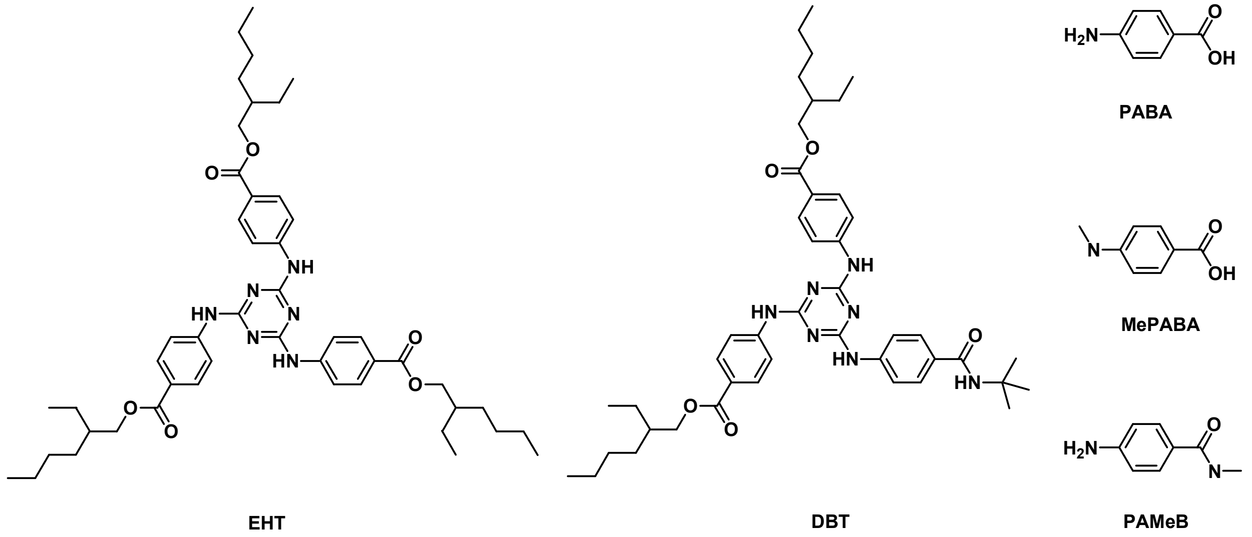

Scheme 1 Molecular structures of EHT, DBT, PABA, MePABA and PAMeB.

In the present study, we observed the UV absorption, triplet–triplet (T–T) absorption, fluorescence, phosphorescence and electron paramagnetic resonance (EPR) spectra of EHT and DBT in ethanol. We determined the energy levels of the S_1 and T_1 states. We also determined the lifetimes and zero-field splitting (ZFS) parameters of the T_1 states in ethanol at 77 K. Photosensitized production of singlet oxygen by EHT and DBT was observed in ethanol at room temperature. The photoexcited T_1 states of *p*-(*N*-methylamino)benzoic acid (MePABA, Scheme 1) and *p*-amino-*N*-methylbenzamide (PAMeB, Scheme 1) have been studied for comparison. The nature of the T_1 states of EHT and DBT is discussed.

Experimental

Chemicals

EHT (BASF), DBT (Fluka), MePABA (TCI EP Grade), PAMeB (TCI), Rose Bengal (Wako Special Grade), phenalenone (Aldrich), acetonitrile (Wako Special Grade) and ethanol (Wako Super Special Grade) were used as received. Although measurements were carried out at room temperature and at 77 K, the concentrations shown in this study were determined at room temperature. The concentrations should be corrected for shrinkage of the solution upon freezing at 77 K. For T–T absorption decay measurements, sample solutions were deaerated by freeze–pump–thaw cycles.

Optical and EPR measurements

The UV absorption spectra were measured with a JASCO V-550 spectrometer. The UV absorption spectra at 77 K were measured by the same method as described previously.[27,28] The fluorescence, fluorescence–excitation and phosphorescence–excitation spectra were measured with a JASCO FP-6500 spectrofluorometer. For the phosphorescence measurements, samples were excited with an Asahi Spectra REX-250 Hg lamp (250 W) equipped with an interference filter (313 nm), an Asahi Technoglass UV-D33S glass filter (transmits the wavelength 250–400 nm), the 5 cm of nonfluorescent water and a Copal DC-494 electromechanical shutter. The emissions from a sample were passed through a Horiba Jobin Yvon H-20VIS spectrometer and detected by a Hamamatsu Photonics R374 photomultiplier tube equipped with a Hamamatsu Photonics C7319 amplifier unit (DC~20 kHz). The output signal was recorded with a Keyence NR-2000 data acquisition system for the phosphorescence spectra. In the decay measurements, the output signal was fed into a Tektronix TDS 3012C digital oscilloscope (100 MHz) and data were averaged. Fluorescence decay profiles were obtained by using a Horiba NAES-700F time-resolved photoluminescence spectrometer with a flash lamp used as an excitation light source.

The time-resolved T–T absorption measurements were carried out in ethanol at 25°C. Samples were excited with a Continuum Surelite Nd:YAG laser (266 nm, repetition rate 10 Hz) equipped with the UV-D33S glass filter. The sample solution was flowed in a Tosoh T-57-UV-10 cuvette (10 mm optical path length). An Asahi Spectra Max-302 Xe lamp (300 W) was used as a probe light source. The white probe light was passed through a Horiba Jobin Yvon H-20UV spectrometer and detected by the Hamamatsu Photonics R374 photomultiplier tube equipped with a Hamamatsu Photonics C9999 amplifier unit (DC~10 MHz). The output signal was recorded with a Stanford Research SR250 boxcar integrator and the Keyence NR-2000 data acquisition system for the T–T absorption spectra. The output signal was also fed into the Tektronix TDS 3012C digital oscilloscope and transferred to a personal computer in the time-profile measurements.

The time-resolved near-IR emission measurements were carried out in ethanol and in acetonitrile at 25°C with the Continuum Surelite Nd:YAG laser (266 nm, 355 nm and 532 nm) used as an excitation light source. The emissions were passed through a Shimadzu SPG-120IR and then detected by a Hamamatsu Photonics H10330A-45 near-IR photomultiplier tube module equipped with the Hamamatsu Photonics C9999 amplifier unit. The output signal was fed into the Tektronix TDS 3012C digital oscilloscope and the Stanford Research SR250 boxcar integrator.

The EPR spectra were measured in ethanol at 77K by a JEOL-JES-FE1XG X-band spectrometer. The static magnetic field was calibrated with an Echo Electronics EFM-2000 proton NMR gauss meter equipped with an EFM-1P probe. Samples were excited with a Canrad-Hanovia Xe-Hg lamp of 1 kW run

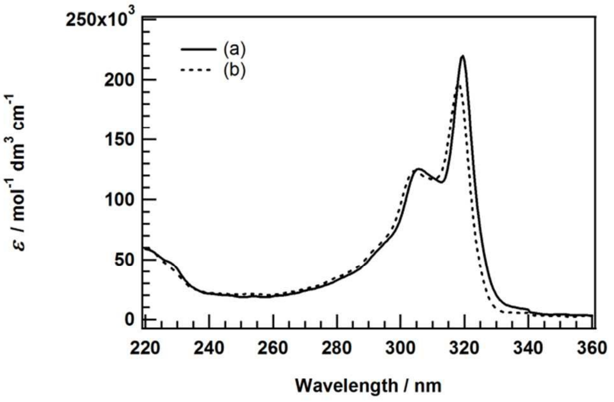

Fig. 1 UV absorption spectra of (a) EHT and (b) DBT in ethanol at 77 K. The sample solutions were prepared at a concentration of 3×10^{-4} mol dm^{-3}.

at 500 W equipped with the same glass filter, water and electromechanical shutter as used for the phosphorescence measurements. To improve the signal-to-noise ratio, the EPR signals were accumulated by using an Electronica ELK-5125-1 waveform storage and a personal computer system.

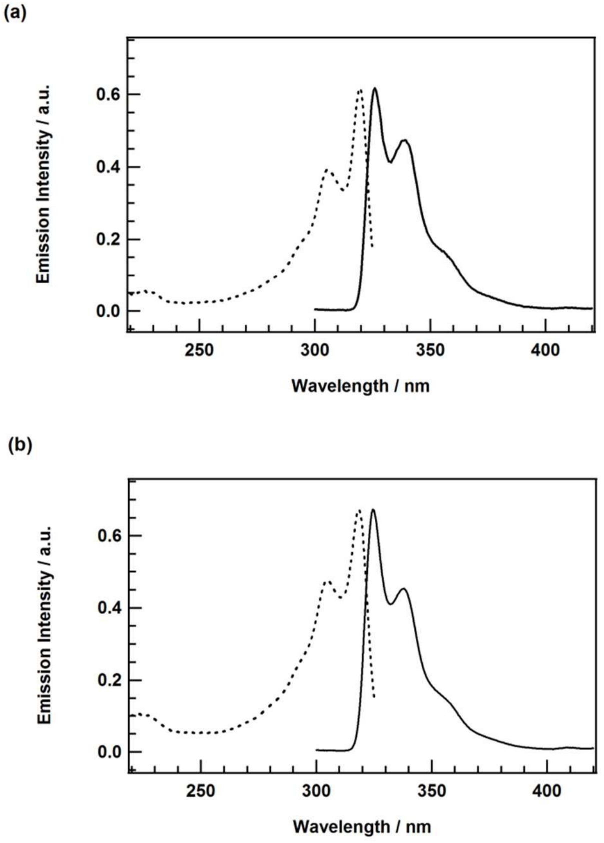

Fig. 2 Fluorescence (full line, $\lambda_{exc} = 280$ nm) and fluorescence–excitation (dotted line, $\lambda_{obs} = 340$ nm) spectra of (a) EHT and (b) DBT in ethanol at 77 K. The sample solutions were prepared at a concentration of 9×10^{-6} mol dm^{-3} and 9×10^{-7} mol dm^{-3} for the fluorescence and fluorescence–excitation measurements, respectively.

Results and discussion

UV absorption and emission spectra

The UV absorption spectra of EHT and DBT were measured in ethanol at 25 °C and 77 K. The spectrum of EHT observed at 77 K shows two peaks in the UV-B range, as shown in Fig. 1. On the other hand, the spectrum observed at 25 °C shows somewhat blurred vibrational structure and only one peak at 314 nm in the UV-B range as reported by Douarre *et al*. and Herzog *et al*.[10,21] The molar absorption coefficients of EHT and DBT in ethanol at 25 °C were obtained to be 130 000 mol^{-1} dm^3 cm^{-1} at 314 nm and 110 000 mol^{-1} dm^3 cm^{-1} at 311 nm, respectively. It should be mentioned here that the molar absorption coefficients of EHT and DBT significantly increase at 77 K. In the analysis of data, the concentrations were corrected for shrinkage of the solution upon freezing at 77 K (20% by volume).[29,30] The molar absorption coefficients of EHT and DBT in ethanol at 77 K thus obtained are 220 000 mol^{-1} dm^3 cm^{-1} at 319 nm and 190 000 mol^{-1} dm^3 cm^{-1} at 318 nm, respectively.

Fig. 2a shows the fluorescence and fluorescence–excitation spectra of EHT in ethanol at 77 K. The fluorescence–excitation spectrum is similar to the UV absorption spectrum shown in Fig. 1a. This fact shows that the observed fluorescence spectrum can be regarded as a fluorescence spectrum of EHT. The energy level of the S_1 state of EHT was estimated to be 31 100 cm^{-1} from the intersection point of the UV absorption and fluorescence spectra.[31] Fig. 2b shows the fluorescence and

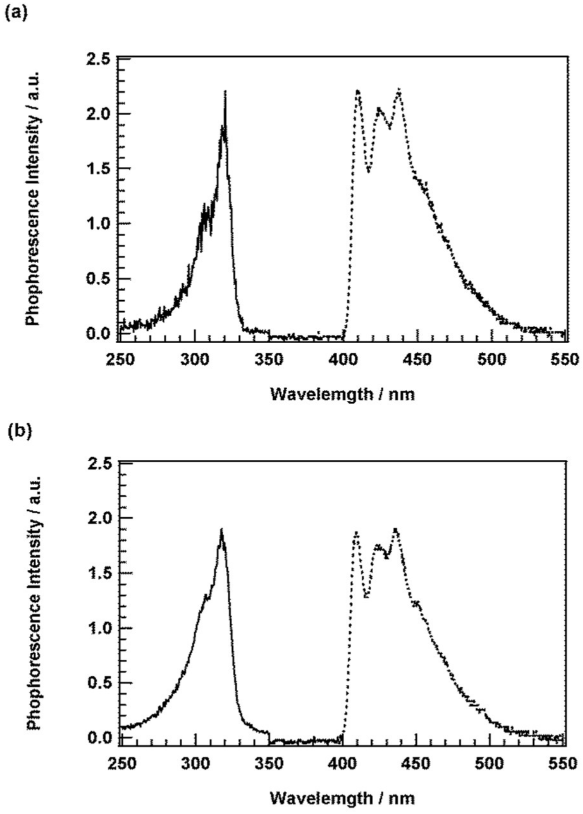

Fig. 3 Phosphorescence (dotted line, $\lambda_{exc} = 313$ nm) and phosphorescence–excitation (full line, $\lambda_{obs} = 410$ nm) spectra of (a) EHT and (b) DBT in ethanol at 77 K. The sample solutions were prepared at a concentration of 3×10^{-6} mol dm^{-3} and 9×10^{-7} mol dm^{-3} for the phosphorescence and phosphorescence–excitation measurements, respectively.

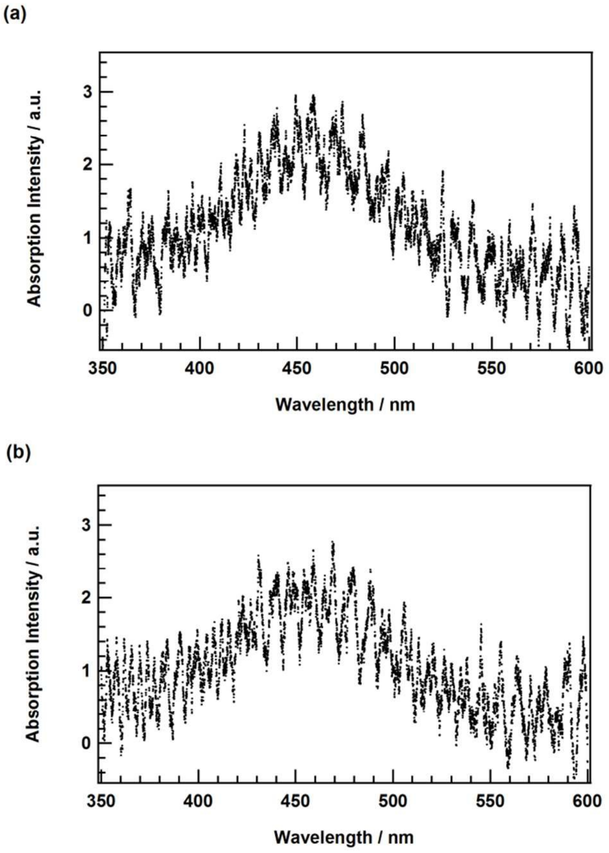

Fig. 4 Transient absorption spectra of (a) EHT and (b) DBT in Ar-saturated ethanol at 25 °C. The sampling times were set at 3–8 μs after the 266 nm YAG laser pulse. The sample solutions were prepared at a concentration of 5 × 10^{-5} mol dm^{-3} (absorbance at 266 nm was 1.0).

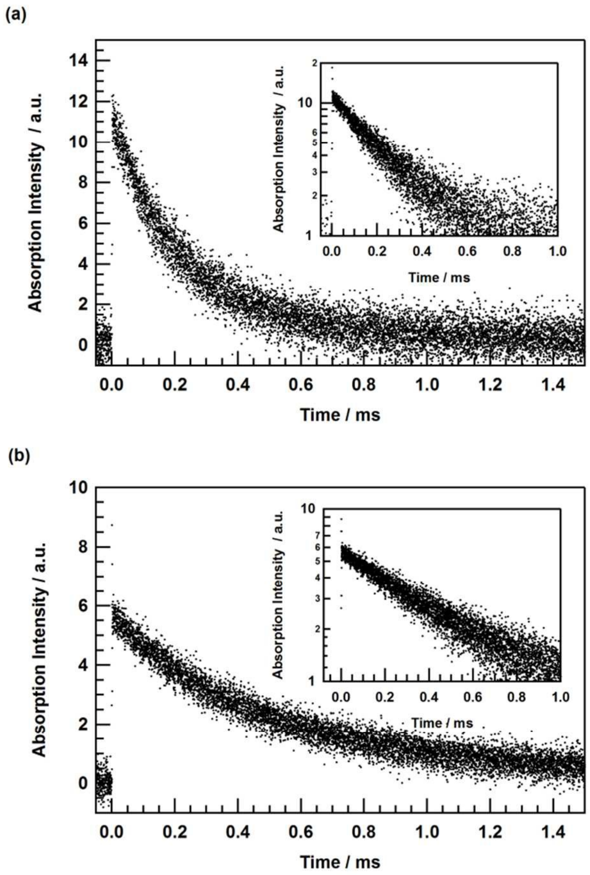

Fig. 5 Time profiles of the transient absorption of (a) EHT and (b) DBT in deaerated ethanol at 25 °C. Transient absorption was monitored at (a) 460 nm and (b) 470 nm. The sample solutions were prepared at a concentration of 5 × 10^{-5} mol dm^{-3}.

fluorescence–excitation spectra of DBT in ethanol at 77 K. In the same manner as for EHT, the energy level of the S_1 state of DBT was estimated to be 31 200 cm^{-1}. The decay of fluorescence of both EHT and DBT could not be resolved from the instrument response function, indicating their S_1 lifetimes of shorter than 0.6 ns in ethanol.

The phosphorescence and phosphorescence–excitation spectra of EHT and DBT were measured in ethanol at 77 K, as shown in Fig. 3. The phosphorescence–excitation spectra are similar to the UV absorption spectra shown in Figs. 1a and 1b. These facts show that the observed phosphorescence spectra can be regarded as phosphorescence spectra of EHT and DBT. The energy levels of the T_1 states of EHT and DBT were estimated to be 24 000 cm^{-1} and 24 200 cm^{-1} from the first peak of phosphorescence, respectively. The T_1 energies of EHT and DBT are higher than that of the enol form of 4-*tert*-butyl-4'-methoxydibenzoylmethane (BMDBM, avobenzone, Parsol 1789), the most widely used UV-A absorber, 20 400 cm^{-1}.[27] EHT and DBT may act as a triplet-energy donor for photounstable BMDBM in the mixture of BMDBM and EHT or DBT. The lifetimes of the T_1 states of both EHT and DBT obtained from the decay of the first peak of phosphorescence are 2.1 s.

The quantum yields of fluorescence (Φ_F) of EHT and DBT were determined relative to 9,10-diphenylanthracene in ethanol at 25 °C and at 77 K, Φ_F = 0.95 and Φ_F = 1.00, respectively.[30,32,33] Φ_F values of EHT and DBT obtained in ethanol at 25 °C are 0.17 and 0.031, respectively. At 77 K, the total emissions at wavelengths longer than 400 nm are composed of fluorescence and phosphorescence. In the same manner as reported previously,[34] the intensity ratios of phosphorescence (I_P) to fluorescence (I_F) of EHT and DBT were determined to be $I_P/I_F = 0.37$ at 409 nm and $I_P/I_F = 0.46$ at 410 nm, respectively. From these intensity ratios the fluorescence spectra were separated from the total emission spectra. From the corrected fluorescence spectra, Φ_F values of EHT and DBT were determined to be 0.57 and 0.68, respectively. Both EHT and DBT are strongly fluorescent in ethanol at 77 K. From the corrected fluorescence and phosphorescence spectra, the quantum yield ratios of phosphorescence (Φ_P) to Φ_F were estimated to be Φ_P/Φ_F = 0.030 and 0.021 for EHT and DBT, respectively. As a result, the values of Φ_P were determined to be 0.017 and 0.014 for EHT and DBT, respectively.

Transient absorption spectra

To obtain the spectral and kinetic information of the triplet states at room temperature, the transient absorption spectra of EHT and DBT were measured by using laser flash photolysis in ethanol at 25 °C. Fig. 4 shows the transient absorption spectra of EHT and DBT in Ar-saturated ethanol obtained 3–8 μs after the 266 nm laser pulse. Fig. 5 shows the time profiles of the

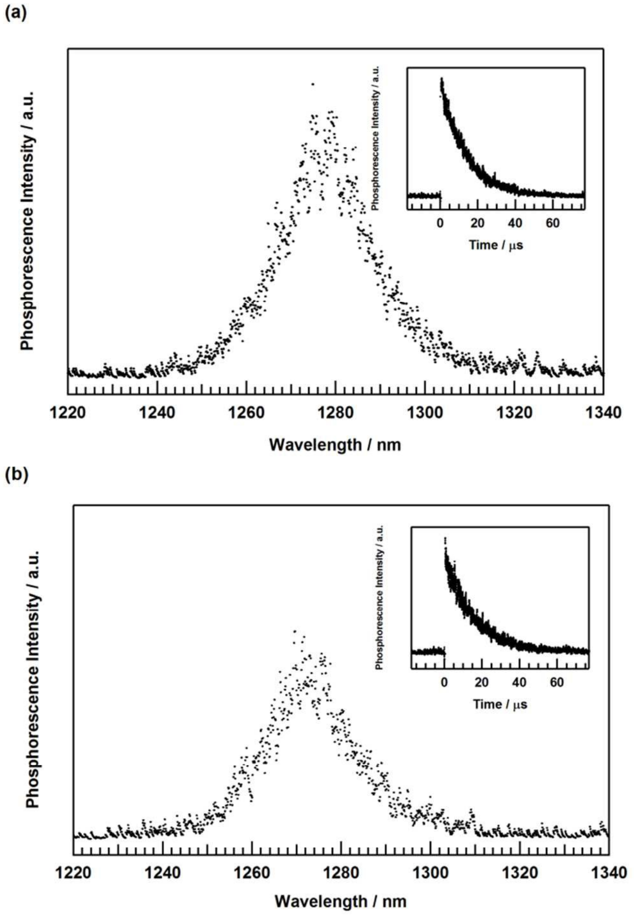

Fig. 6 Time-resolved near-IR phosphorescence spectra of singlet oxygen, $^1O_2(^1\Delta_g)$, generated by excitation of (a) EHT and (b) DBT in oxygen-saturated ethanol with 266 nm YAG laser pulses at 25 °C. The sampling times were set at 5–20 µs after the laser pulse. Inset: the phosphorescence intensity was monitored at 1274 nm. The sample solutions were prepared at a concentration of 5×10^{-5} mol dm^{-3}.

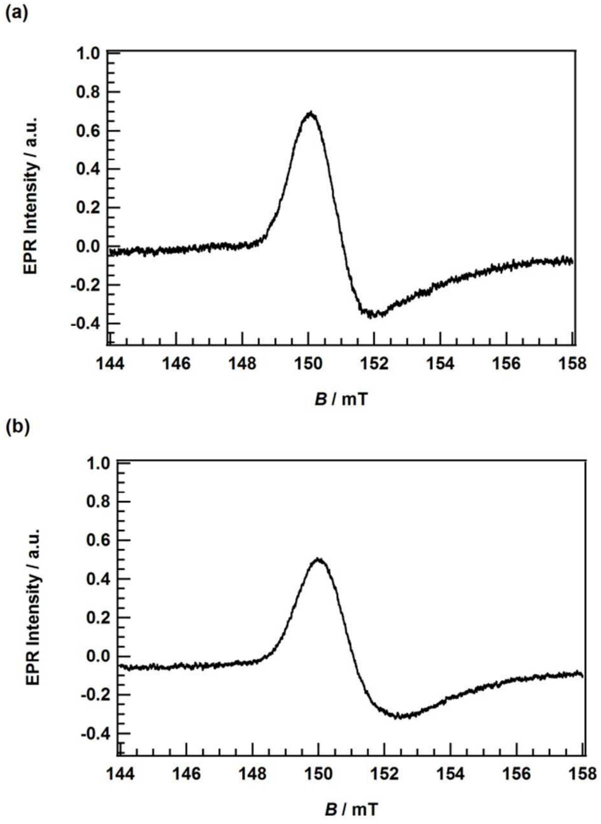

Fig. 7 EPR spectra of (a) EHT and (b) DBT in ethanol at 77 K. The sample solutions were prepared at a concentration of 3×10^{-3} mol dm^{-3}.

transient absorption signals of EHT and DBT. The lifetimes of the transient species were significantly reduced in the presence of ground-state oxygen, $^3O_2$, which is a well-known triplet quencher.[35] The observed transient spectra can be reasonably assigned to T–T absorption spectra. The T–T absorption decays were exponential, and the lifetimes of the T_1 states of EHT and DBT were estimated to be 250 µs and 550 µs in deaerated ethanol at 25 °C, respectively.

Time-resolved near-IR phosphorescence spectra of singlet oxygen

Quenching of an excited triplet state of an organic molecule by $^3O_2$ generally follows energy transfer to produce singlet oxygen, $^1O_2(^1\Delta_g)$, and/or formation of a peroxide.[35] The near-IR phosphorescence spectra of $^1O_2(^1\Delta_g)$ generated by photosensitization with EHT and DBT were measured in oxygen-saturated ethanol at 25 °C, as shown in Fig. 6. The phosphorescence peak was observed at 1274 nm. The lifetimes of $^1O_2(^1\Delta_g)$ generated by excitation of EHT and DBT were determined to be 14.5 µs and 16.2 µs, respectively. The observed wavelength of the phosphorescence peak is very close to that reported by Schmidt.[36] The observed lifetimes are close to those observed in ethanol by Shimizu *et al.* and Kikuchi *et al*.[37,38]

The quantum yields of $^1O_2(^1\Delta_g)$ generation, Φ_Δ, were determined relative to phenalenone in oxygen-saturated ethanol because Φ_Δ generated by phenalenone was reported to be almost unity in many solvents including methanol.[39,40] The values of Φ_Δ were determined to be 0.11 and 0.023 for EHT and DBT, respectively.

Interactions of $^1O_2(^1\Delta_g)$ with an organic molecule such as β–carotene result in the quenching of $^1O_2(^1\Delta_g)$.[35] We tried to estimate the rate constants for the quenching of $^1O_2(^1\Delta_g)$, k_Q, by EHT and DBT. Using phenalenone and Rose Bengal as photosensitizer, $^1O_2(^1\Delta_g)$ was generated with 266 nm, 355 nm and 532 nm YAG laser pulses in ethanol and in acetonitrile at 25 °C in the presence of EHT and DBT. However, the lifetime of $^1O_2(^1\Delta_g)$ was not reduced in the presence of EHT (2.5×10^{-3} mol dm^{-3}) and DBT (5.0×10^{-3} mol dm^{-3}). The lifetime of $^1O_2(^1\Delta_g)$ generated by excitation of phenalenone (1.0×10^{-4} mol dm^{-3}) is 79 µs in acetonitrile. These facts indicate that the k_Q values by EHT and DBT are smaller than 5.1×10^5 mol^{-1} dm^3 s^{-1} and 2.5×10^5 mol^{-1} dm^3 s^{-1}, respectively.

In contrast to the present study, Lhiaubet-Vallet *et al.* reported that EHT and DBT exhibited an important potential to quench $^1O_2(^1\Delta_g)$ in acetonitrile.[41] They used an excimer laser (308 nm) for excitation and the k_Q values by EHT and DBT were determined to be 4×10^8 mol^{-1} dm^3 s^{-1} and 1.8×10^8 mol^{-1} dm^3 s^{-1}, respectively.[41] At the present stage of this study, we do not elucidate the exact reasons for the discrepancy in antioxidative properties between the present study and the

Table 1 Molar absorption coefficients (ε), S_1 energies (E_{S1}), T_1 energies (E_{T1}), quantum yields (Φ), zero-field splitting parameters (D^*) and T_1 lifetimes (τ) observed in ethanol at 77 K

Molecule	ε (mol^{-1} dm^3 cm^{-1})	E_{S1} (cm^{-1})	E_{T1} (cm^{-1})	Φ_F	Φ_P	D^* (cm^{-1})	τ_P (s) [a]	τ_{EPR} (s) [b]
EHT	220 000 (at 319 nm)	31 100	24 000	0.57	0.017	0.1064	2.1	2.1
DBT	190 000 (at 318 nm)	31 200	24 200	0.68	0.014	0.1042	2.1	2.1
MePABA	20 000 (at 300 nm) [c]	30 900	23 800	0.20	0.091	0.1005	3.0	2.8
PAMeB	18 300 (at 280 nm) [c]	31 500	24 100	0.16	0.067	0.1007	2.8	2.6

[a] Obtained from the decay of phosphorescence. [b] Obtained from the decay of the EPR B_{min} signal. [c] Observed at 298 K.

report by Lhiaubet-Vallet *et al*. However, one possible explanation for the discrepancy is that the molar absorption coefficients of EHT and DBT are very large at 308 nm and the generated $^1O_2(^1\Delta_g)$ molecules were efficiently quenched by the T_1 states of EHT and DBT.

The values of k_Q by MePABA and PAMeB were determined for comparison. The lifetime of $^1O_2(^1\Delta_g)$ generated by excitation of phenalenone was measured in acetonitrile by changing the concentrations of MePABA and PAMeB. The results are given in Figs. S1 and S2. The k_Q values by MePABA and PAMeB were estimated to be 1.7×10^6 mol^{-1} dm^3 s^{-1} and 1.3×10^6 mol^{-1} dm^3 s^{-1}, respectively.

Magnetic properties of the triplet state

Assuming the isotropic g value, the magnetic fine structure of the triplet state in the presence of an external magnetic field $\boldsymbol{B}$ can be described by the following spin Hamiltonian:

$$\begin{aligned} H_S &= g\mu_B \boldsymbol{B}\bullet\boldsymbol{S} + \boldsymbol{S}\bullet\boldsymbol{D}\bullet\boldsymbol{S} \\ &= g\mu_B \boldsymbol{B}\bullet\boldsymbol{S} - XS_x^2 - YS_y^2 - ZS_z^2 \\ &= g\mu_B \boldsymbol{B}\bullet\boldsymbol{S} + D[S_z^2 - (1/3)\boldsymbol{S}^2] + E(S_x^2 - S_y^2). \end{aligned} \tag{1}$$

Here, $-X$, $-Y$, and $-Z$ are the principal values of the $\boldsymbol{D}$ tensor (ZFS tensor), and D and E are the ZFS parameters. The other symbols have their usual meaning. The ZFS parameters D, E and D^* are defined to be $D = -3Z/2$, $E = (Y - X)/2$ and $D^* = (D^2 + 3E^2)^{1/2}$. The D^* value can be obtained from the observed resonance field of B_{min} signal with Kottis and Lefebvre's correction with the aid of the following equation:[42]

$$D^* = \{(3/4)(h\nu)^2 - 3(g\mu_B B_{min})^2\}^{1/2}, \tag{2}$$

where, h and ν have their conventional meanings.

The EPR spectra of the T_1 states of EHT and DBT were measured in ethanol at 77 K, as shown in Fig. 7. Assuming the isotropic g value to be equal to the free electron value, the D^* values were obtained and are listed in Table 1. The T_1 lifetimes obtained from the decay of the EPR B_{min} signal are also listed in Table 1. The T_1 lifetimes obtained from the EPR measurements are in good agreement with those obtained from the phosphorescence measurements. This agreement shows that the observed EPR spectra are reasonably assigned to the EPR spectra of the T_1 states of EHT and DBT.

Nature of the lowest excited triplet states

EHT and DBT are strongly fluorescent in the S_1 states and phosphorescent in the T_1 states in ethanol at 77 K. The EPR B_{min} signals of the T_1 states were observed. These facts show that the deactivation process is predominantly fluorescence, however, a significant portion of the S_1 molecules undergoes intersystem crossing to the T_1 state at 77 K.

At room temperature, the T–T absorption spectra of EHT and DBT and phosphorescence spectra of $^1O_2(^1\Delta_g)$ generated by photosensitization with EHT and DBT were observed. These facts also show that a significant portion of the S_1 molecules undergoes intersystem crossing to the T_1 state at room temperature, although we do not have the accurate data on the quantum yield of the $S_1 \rightarrow T_1$ intersystem crossing.

The Φ_Δ values at room temperature are 0.11 and 0.023 for EHT and DBT, respectively. As is known, the $^3\pi\pi^*$ states of aromatic molecules are generally high efficient at producing $^1O_2(^1\Delta_g)$, frequently with $S_\Delta \geq 0.8$.[35] Here, S_Δ is the fraction of triplet quenching events that results in the formation of $^1O_2(^1\Delta_g)$.[34] Therefore, the quantum yields of the $S_1 \rightarrow T_1$ intersystem crossing may be assumed to be about 0.14 and 0.029 for EHT and DBT at room temperature, respectively. As is mentioned above, the Φ_F values of EHT and DBT significantly decrease at room temperature. This fact indicates an increase in the rate constant of the internal conversion at room temperature. The deactivation process is predominantly internal conversion for both EHT and DBT at room temperature.

The lifetimes of the T_1 states of EHT and DBT are about 2 s and the D^* values are about 0.1 cm^{-1}. These values suggest that the T_1 states of EHT and DBT possess mainly a $^3\pi\pi^*$ character in ethanol. To study the T_1 states of EHT and DBT in detail, the emission, phosphorescence and EPR spectra of MePABA and PAMeB were observed in ethanol at 77 K. The results are given in Table 1 and Figs. S3–S5. The observed T_1 energy and T_1 lifetime of MePABA are close to those observed in EPA (diethyl ether, isopentane and ethanol, 5:5:2 by volume) at 77 K.[43]

As is clearly seen in Table 1, the energy level, lifetime and D^* value of the T_1 state of EHT are similar to those of MePABA. The T_1 state of EHT can reasonably be assigned to a locally excited triplet state within MePABA, and the two unpaired electrons of EHT in the T_1 state localize on the MePABA fragment. In the same manner as for EHT, the T_1 state of DBT can reasonably be assigned to a locally excited triplet state within MePABA or PAMeB.

Conclusions

The observed T_1 energies, T_1 lifetimes and ZFS parameters indicate that the T_1 state of EHT can be assigned to a locally excited $^3\pi\pi^*$ state within MePABA, while the T_1 state of DBT can be assigned to a locally excited $^3\pi\pi^*$ state within MePABA or PAMeB. In ethanol at 77 K, fluorescence is dominant among the deactivation processes of the S_1 states of EHT and DBT, however, a significant portion of the S_1 molecules undergoes intersystem crossing to the T_1 states. The near-IR phosphorescence spectra of $^1O_2(^1\Delta_g)$ generated by photosensitization with EHT and DBT were observed in ethanol at room temperature. EHT and DBT did not exhibit significantly antioxidative properties by quenching singlet oxygen.

Acknowledgements

This work was supported in part by Grants-in-Aid for Scientific Research (A) (No. 23241034) and for Exploratory Research (No. 24655060) from the Ministry of Education, Culture, Sports, Science and Technology (MEXT) and the Japan Society for the Promotion of Science (JSPS). This work was also supported in part by Takahashi Industrial and Economic Research Foundation.

Notes and references

[a] *Department of Chemistry, Graduate School of Engineering, Yokohama National University, Tokiwadai, Hodogaya-ku, Yokohama 240-8501, Japan. E-mail: akikuchi@ynu.ac.jp, yagimiki@ynu.ac.jp*

[b] *Shiseido Research Center, Hayabuchi, Tsuzuki-ku, Yokohama 224-8558, Japan*

Electronic Supplementary Information (ESI) available: Stern-Volmer plots of the phosphorescence lifetime of singlet oxygen in acetonitrile at room temperature. The emission, phosphorescence and EPR spectra of MePABA and PAMeB in ethanol at 77 K. See DOI: 10.1039/b000000x/

1 N. Serpone, A. Salinaro, A. V. Emeline, S. Horikoshi, H. Hidaka and J. Zhao, An *in vitro* systematic spectroscopic examination of the photostabilities of a random set of commercial sunscreen lotions and their *chemical* UVB/UVA active agents, *Photochem. Photobiol. Sci.*, 2002, **1**, 970–981.

2 M. D. Palm and M. N. O'Donoghue, Update on photoprotection, *Dermatol. Ther.*, 2007, **20**, 360–376.

3 K. Klein and I. Palefsky, Formulating sunscreen products, in *Sunscreens*, ed. N. A. Shaath, Taylor & Francis, Boca Raton, 2005, pp. 353–383.

4 D. C. Steinberg, Regulations of sunscreens worldwide, in *Sunscreens*, ed. N. A. Shaath, Taylor & Francis, Boca Raton, 2005, pp. 173–198.

5 D. R. Sambandan and D. Ratner, Sunscreens: An overview and update, *J. Am. Acad. Dermatol.*, 2011, **64**, 748–758.

6 B. Herzog, D. Hueglin and U. Osterwalder, New sunscreen actives, in *Sunscreens*, ed. N. A. Shaath, Taylor & Francis, Boca Raton, 2005, pp. 291–320.

7 J. D. Bos and M. M. H. M. Meinardi, The 500 Dalton rule for the skin penetration of chemical compounds and drugs, *Exp. Dermatol.*, 2000, **9**, 165–169.

8 N. A. Shaath, Global developments in sun care ingredients, *Cosmet. Toiletries*, 2006, **121**, 57–66.

9 N. A. Shaath, Ultraviolet filters, *Photochem. Photobiol. Sci.*, 2010, **9**, 464–469.

10 L. Douarre, R. Arnaud, J. Lemaire, A. Deflandre and H. Richard, Photochemical study of substituted *s*-triazines, *J. Photochem. Photobiol., A,* 1996, **96**, 71–78.

11 C. A. Bonda, The photostability of organic sunscreen actives: A review, in *Sunscreens*, ed. N. A. Shaath, Taylor & Francis, Boca Raton, 2005, pp. 321–349.

12 C. A. Bonda, A. Pavlovic, K. Hanson and C. Bardeen, Singlet quenching proves faster is better for photostability, *Cosmet. Toiletries*, 2010, **125**, 40–48.

13 A. Kikuchi and M. Yagi, Direct observation of the intermolecular triplet-triplet energy transfer from UV-A absorber 4-*tert*-butyl-4'-methoxydibenzoylmethane to UV-B absorber octyl methoxycinnamate, *Chem. Phys. Lett.*, 2011, **513**, 63–66.

14 A. Kikuchi, H. Saito, M. Mori and M. Yagi, Photoexcited triplet states of new UV absorbers, cinnamic acid 2-methylphenyl esters, *Photochem. Photobiol. Sci.*, 2011, **10**, 1902–1909.

15 J. Kockler, M. Oelgemöller, S. Robertson and B. D. Glass, Photostability of sunscreens. *J. Photochem. Photobiol., C,* 2012, **13**, 91–110.

16 N. Oguchi-Fujiyama, K. Miyazawa, A. Kikuchi and M. Yagi, Photophysical properties of dioctyl 4-methoxybenzylidenemalonate: UV-B absorber, *Photochem. Photobiol. Sci.*, 2012, **11**, 1528–1535.

17 A. Kikuchi, N. Oguchi-Fujiyama, K. Miyazawa and M. Yagi, Triplet–triplet energy transfer from a UV-A absorber butylmethoxydibenzoylmethane to UV-B absorbers, *Photochem. Photobiol.*, 2014, **90**, 511–516.

18 S. Sommer, S. M. Wilkinson, J. S. C. English and J. Ferguson, Photoallergic contact dermatitis from the sunscreen octyl triazone, *Contact Dermatitis*, 2002, **46**, 304–305.

19 E. Damiani, W. Baschong and L. Greci, UV-Filter combinations under UV-A exposure: Concomitant quantification of over-all spectral stability and molecular integrity, *J. Photochem. Photobiol., B*, 2007, **87**, 95–104.

20 C. Couteau, A. Faure, J. Fortin, E. Paparis and L. J. M. Coiffard, Study of the photostability of 18 sunscreens in creams by measuring the SPF in vitro, *J. Pharm. Biomed. Anal.*, 2007, **44**, 270–273.

21 B. Herzog, M. Wehrle and K. Quass, Photostability of UV absorber systems in sunscreens, *Photochem. Photobiol.*, 2009, **85**, 869–878.

22 A. C. Kerr, B. Niklasson, R. S. Dawe, A. –M. Escoffier, M. Krasteva, B. Sanderson and J. Ferguson, A double-blind, randomized assessment of the irritant potential of sunscreen chemical dilutions used in photopatch testing, *Contact Dermatitis*, 2009, **60**, 203–209.

23 A. Kerr and J. Ferguson, Photoallergic contact dermatitis, *Photodermatol. Photoimmunol. Photomed.*, 2010, **26**, 56–65.

24 J. Hojerová, A. Medovcíková and M. Mikula, Photoprotective efficacy and photostability of fifteen sunscreen products having the

same label SPF subjected to natural sunlight, *Int. J. Pharm.*, 2011, **408**, 27–38.

25 B. L. Diffey and M. W. Brown, The ideal spectral profile of topical sunscreens, *Photochem. Photobiol.*, 2012, **88**, 744–747.

26 The European Multicentre Photopatch Test Study (EMCPPTS) Taskforce, A European multicentre photopatch test study, *Br. J. Dermatol.*, 2012, **166**, 1002–1009.

27 A. Kikuchi, N. Oguchi and M. Yagi, Optical and electron paramagnetic resonance studies of the excited states of 4-*tert*-butyl-4'-methoxydibenzoylmethane and 4-*tert*-butyl-4'-methoxydibenzoylpropane, *J. Phys. Chem., A*, 2009, **113**, 13492–13497.

28 R. Kumasaka, A. Kikuchi and M. Yagi, Photoexcited states of UV absorbers, benzophenone derivatives, *Photochem. Photobiol.*, 2014, **90**, 727–733.

29 R. Passerini and I. G. Ross, An apparatus for the ultra-violet spectroscopy of solutions at low temperatures, *J. Sci. Instrum.*, 1953, **30**, 274–276.

30 M. Montalti, A. Credi, L. Prodi and M. T. Gandolfi, *Handbook of photochemistry, 3rd ed.*, Tayler & Francis, Boca Raton, 2006.

31 Z. R. Grabowski and A. Grabowska, The Förster cycle reconsidered, *Z. Physik. Chem., Neue Folge*, 1976, **101**, 197–208.

32 G. Heinrich, S. Schoof and H. Gusten, 9,10-Diphenylanthracene as a fluorescence quantum yield standard, *J. Photochem.*, 1974–1975, **3**, 315–320.

33 J. V. Morris, M. A. Mahaney and J. R. Huber, Fluorescence quantum yield determinations. 9,10-Diphenylanthracene as a reference standard in different solvents, *J. Phys. Chem.*, 1976, **80**, 969–974.

34 A. Kikuchi, K. Shibata, R. Kumasaka and M. Yagi, Excited states of menthyl anthranilate: a UV-A absorber, *Photochem. Photobiol. Sci.*, 2013, **12**, 246–253.

35 N. J. Turro, V. Ramamurthy and J. C. Scaiano, *Modern Molecular Photochemistry of Organic Molecules*, Unversity Science Books, Sausalito, 2010.

36 R. Schmidt, Solvent Shift of the $^1\Delta_g \rightarrow {}^3\Sigma_g^-$ phosphorescence of O_2, *J. Phys. Chem.*, 1996, **100**, 8049–8052.

37 O. Shimizu, J. Watanabe, K. Imakubo and S. Naito, Absolute quantum yields and lifetimes of photosensitized phosphorescence of singlet oxygen O_2 ($^1\Delta_g$) in air-saturated aqueous and organic solutions of phenalenone, *Chem. Lett.*, 1999, **28**, 67–68.

38 A. Kikuchi, K. Shibata, R. Kumasaka and M. Yagi, Optical and time-resolved electron paramagnetic resonance studies of the excited states of a UV-B absorber (4-methylbenzylidene)camphor, *J. Phys. Chem., A*, 2013, **117**, 1413–1419.

39 E. Oliveros, P. Suardi-Murasecco, T. Aminian-Saghafi and A. M. Braun, 1H-Phenalen-1-one: Photophysical properties and singlet-oxygen production, *Helv. Chim. Acta* 1991, **74**, 79–90.

40 R. Schmidt, C. Tanielian, R. Dunsbach and C. Wolff, Phenalenone, a universal reference compound for the determination of quantum yields of singlet oxygen $O_2(^1\Delta_g)$ sensitization, *J. Photochem. Photobiol., A,* 1994, **79**, 11–17.

41 V. Lhiaubet-Vallet, M. Marin, O. Jimenez, O. Gorchs, C. Trullas and M. A. Miranda, Filter-filter interactions. Photostabilization, triplet quenching and reactivity with singlet oxygen, *Photochem. Photobiol. Sci.*, 2010, **9**, 552–558.

42 P. Kottis and R. Lefebvre, Calculation of the electron spin resonance line shape of randomly oriented molecules in a triplet state. I. The $\Delta m = 2$ transition with a constant linewidth, *J. Chem. Phys.*, 1963, **39**, 393–403.

43 T. P. Carsey, G. L. Findley and S. P. McGlynn, Systematics in the electronic spectra of polar molecules. 1. Para-disubstituted benzenes, *J. Am. Chem. Soc.*, 1979, **101**, 4502–4510.